

Design and Development of Single-Pass Beam Position Monitor for TRISTAN Main Ring

M. Arinaga, K. Mori, H. Ishii, T. Naito and M. Tejima

National Laboratory for High Energy Physics (KEK)
Tsukuba, Ibaraki 305, Japan

Abstract

This paper describes the design and development of the single-pass beam position monitor for TRISTAN Main Ring(MR). This system has been developed in compliance with the requirement to measure and detect the beam position every turn-by-turn. At the test run, it caught the decay of beam oscillation.

I. INTRODUCTION

Beam positions in the TRISTAN MR have been measured by the super-heterodyne method. It has many merits. However, it has faults in that it cannot measure the beam position each turn and that it takes a long time to measure COD. This is the reason why this single-pass beam monitor system was designed and developed. One set was constructed and installed in the east symmetrical point section of TRISTAN MR. This monitor adopted, what we call, the AM/PM method, which is based on the amplitude-to-phase conversion.

II. THE OUTLINE OF AM/PM METHOD

There are many methods to realize single-pass beam monitor. We adopted the so-called ratio method which need not normalize resultant signals by the beam power.[1] Button electrodes pick up the beam position signals in this system.

A. The characteristics of AM/PM method

The AM/PM has the following characteristics:

- Electrical circuits treat narrow band signals.
- Using band pass filters, it is strongly resistant to noise.
- The ratio method does not need the normalization process.
- It makes the system a little expensive.

B. The principle of AM/PM method

Figure 1 shows the block diagram of AM/PM method. The calculations are made on signals from two pairs of electrodes separately, the AC-pair and the BD-pair out of four electrode A, B, C, D. As shown in the block diagram, when the beam passes, a signal is generated in each electrode pair, and from the ratios between two signals, the beam position is calculated.

Figure 2 shows a vector diagram to convert amplitude to phase. A band pass filter produces transient sinusoidal ringings from beam signals as shown in Figure 3. The hybrid IC gives them $\pi/2$ phase shifts. The output signals are as follows:

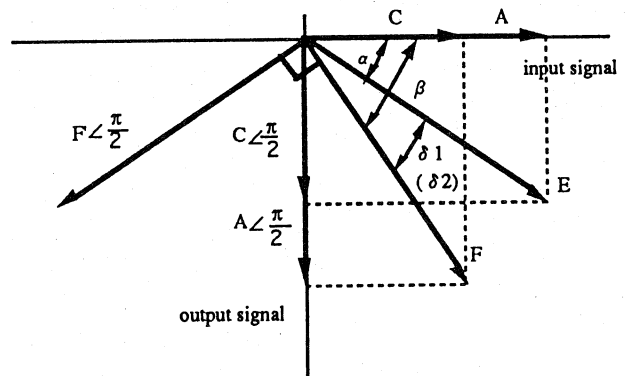


Figure 2 : The vector diagram for changing amplitude to phase difference by $\pi/2$ hybrid IC.

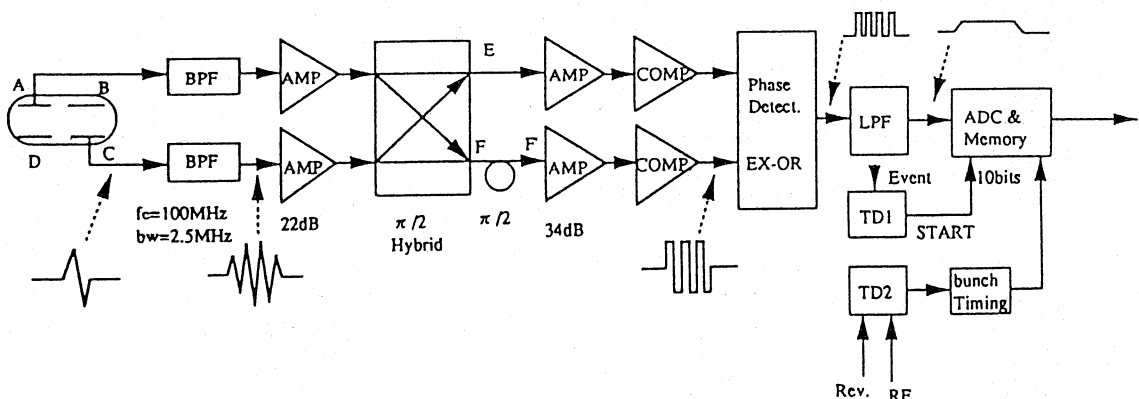


Figure 1 : Block diagram of AM/PM method for TRISTAN main ring.

III. The system description

A. Construction

Construction of the system is shown in Figure 1.

The sampled data are recorded in ADC memories at the timing of each beam, and H80 computer calculates the δx and δy value.

B. Performance

Performance is as following.

- | | |
|------------------------------------|--|
| a. Bands pass filter | $f_0 = 100\text{MHz}$, $\text{bw} = 2.5\text{MHz}$
insertion loss = 2dB |
| b. First amplifier | Wide band($\sim 1.1\text{GHz}$), gain = 22dB
($\mu\text{PC1658C}$, NEC) NF = 2.5dB |
| c. Last amplifier | Wide band($\sim 400\text{MHz}$), high power
(CA2830C, MOTOLORA) gain = 34dB, NF = 3.5dB |
| d. ADC/Mem module | 1.639mV/bit
(AD9020JZ, ANALOG DEVICES) |
| e. Minimum bunch space time | 1 μsec |
| f. Record length | 16384 turns/bunch |
| g. Detectable current range | $I_{\text{beam}} = 0.15\text{mA} \sim 10\text{mA}$ |
| h. $\pi/2$ Hybrid | 87 degrees \sim 93 degrees
(JH-119, anzac) insertion loss = 2dB |
| i. Comparator /PSD | 0 degrees \sim 180 degrees
(MC10H107L, MOTOLORA)
(AD96687BH, ANALOG DEVICES) |
| j. Low Pass Filter | $f_L = 4.4\text{MHz}$ |
| k. 10bits ADC's minimum resolution | $< 50\mu\text{m}$ |

C. Correction of errors and sensitivity

C-1. Errors

There are the following error sources.

- Difference in cable lengths
- Difference in gain of amplifiers
- Difference in phase characteristic and insertion loss of Hybrid ICs
- Difference in phase characteristic of comparators

C-2. Correction and calibration[2]

The errors caused by parts can be minimized by adjustment, if a set with similar performance is available. However, the error caused by the amplifiers cannot be overcome, so the best choice of the amplifier IC is essential. The last, remaining errors can be corrected by software based on calibration of the system.

The calibration of the circuit was performed at the bench-test system. Moving a signal source inside a test chamber, we obtained mapping from the real signal positions into the positions given by the present AM/PM circuit. An example of the mapping is given in Figure 4. Comparing the resultant mapping with that given by the conventional super-heterodyne circuit, we identified individual error sources and corrected them. Some attenuators are inserted in order to make impedance matching. This is useful also to reduce reflection and oscillation in the signal. After trial and error, 3dBs' attenuator is inserted at the front of BPF and $\pi/2$ Hybrid IC at the present. The cable is all semi-rigid cable to avoid the interference oscillation of signal and error. Figure 4, which is

$$E = A + C \angle \frac{\pi}{2},$$

$$F = C + A \angle \frac{\pi}{2},$$

where

$$\tan(\alpha) = \frac{C}{A}, \quad \tan(\beta) = \frac{A}{C},$$

$$\beta + \alpha = \frac{\pi}{2}, \quad \beta - \alpha = \delta 1.$$

We then have

$$\tan\left(\frac{\delta 1}{2}\right) = \tan\left(\frac{\pi}{4} - \alpha\right)$$

$$= \frac{\tan\left(\frac{\pi}{4}\right) - \tan(\alpha)}{1 + \tan\left(\frac{\pi}{4}\right) \times \tan(\alpha)}$$

$$= \frac{A - C}{A + C},$$

$$\frac{\delta 1}{2} = \tan^{-1}\left(\frac{A - C}{A + C}\right).$$

Similar relations hold in the BD-pair:

$$\frac{\delta 2}{2} = \tan^{-1}\left(\frac{B - D}{B + D}\right).$$

Signals proportional to $\delta/2$ are available at the outputs of the phase detectors.

Using the following equations, the position from the center of the chamber is derived:

$$\delta x = \zeta_x \times \frac{\delta 1 - \delta 2}{2},$$

$$\delta y = \zeta_y \times \frac{\delta 1 + \delta 2}{2}.$$

Here, ζ_x and ζ_y are the coefficients of sensitivity characteristic of the types of chamber, an example of which given Figure 4.

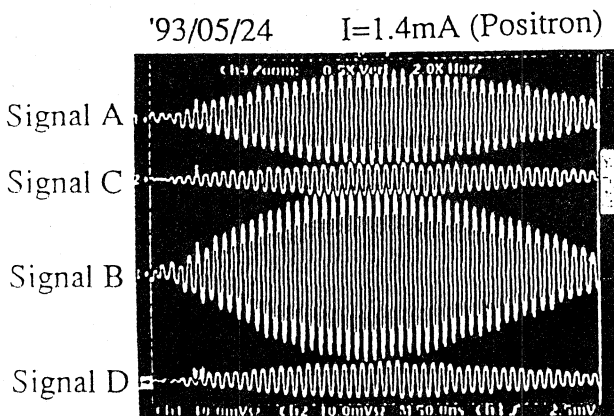


Figure 3 : Ringing signals from BPF.
The vertical scale is 10mV/div.
The horizontal scale is 50nS/div.

an example of mapping and the sensitivity coefficients ζ_x and ζ_y , mentioned section II, respectively gives the conversion coefficient from phase to beam position as 0.235 mm/degree in x direction and 0.239 mm/degree y direction.

Though the old system utilizes 12bit-ADCs, the present system adopts 10bit-ADC. In order to examine the effect of this low resolution, a -50dBm test signal is fed to the test chamber and the resultant ADC outputs are compared exchanging the input electrode pairs.

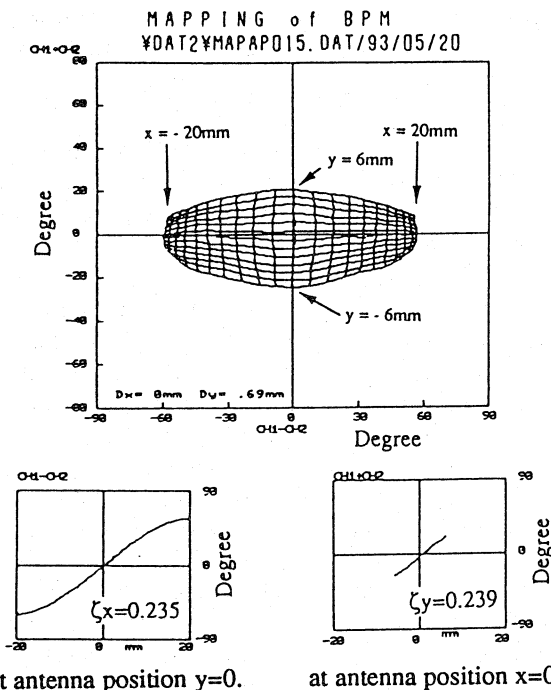


Figure 4 : An example of mapping by AM/PM method. ζ_x , ζ_y are coefficients of sensitivity. D_x , D_y are values of offset from geometrical center. x , y are antenna position

C-3. Sensitivity

After the correction and calibration, this system's gain became 46 dB at the maximum, and the detectable range of beam current was from 0.15mA to 10mA.

C-4. Improvement

We are trying to increase the amplifiers gain to approximately 50dB in order to lower the limit of detectable current range down to 0.1mA.

Output of the PSD, driven by outputs of the comparators in ECL levels, is uni-directional, while the ADC is fabricated so as to mate with bi-directional signals. We are going to insert a level shifter between the PSD and the ADC so that the full range of ADC is efficiently used. This has another advantage, that is, to simplify the data processing because the ADC output becomes zero when the beam is in the normal position.

The present system memorizes only the ADC output to save the time of data storage. It is desirable to save the data in the form of beam position.

IV. PERFORMANCE

Figure. 5 shows the beam oscillation at the injection. According to the FFT analysis made at the injection, both betatron and synchrotron oscillations appear at the injection. The betatron oscillation decays rapidly while the synchrotron oscillation persists. The observation shown in Figure 5 is consistent with the FFT analysis shown in Figure 6. Vertical and horizontal tunes agreed with values measured by another tune-meter.

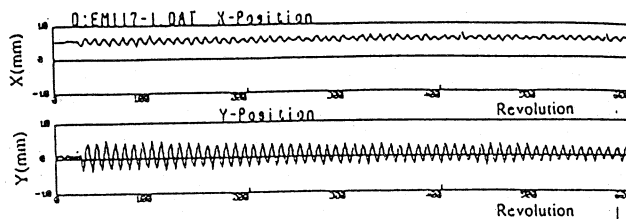


Figure 5 : An example of oscillation of electron beam. This oscillation occurred due to a vertical kicker, when electron beam is circulating at the injection stage.

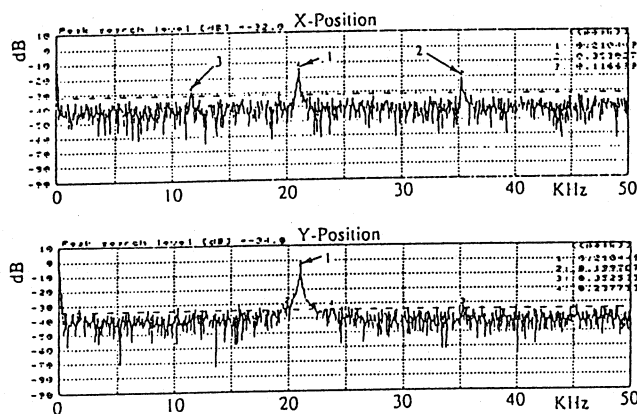


Figure 6 : FFT analysis of electron beam
1. $\nu_x = 35.30\text{KHz}$, 2. $\nu_y = 21.04\text{KHz}$, 3. $\nu_s = 11.67\text{KHz}$

V. CONCLUSION

Development of the single-pass-monitor is very successful. The ability to catch the beam oscillations must extend the application of the beam position monitor.

Four more systems will be installed in the near future, in which improvements suggested in this paper will be made.

VI. REFERENCES

- [1] J. Borer, "Instrumentation and diagnostics used in LEP commissioning, with accent on the LEP beam orbit measurement system", Workshop on Accelerator Instrumentation, F.N.A.L., Batavia, IL, USA, (Oct. 1990), pp. 1-34
- [2] H. Ishii et al, "Beam position monitor system of TRISTAN Main Ring", Proc. Accelerator Science and Technology, Tokyo, Japan, (Oct. 1987), pp.207-209